Naturally Pressurized Gating Systems in Investment Castings

David Poweleit, Diana David - *SFSA*
Rod Grozdanich - *Spokane Industries*
Richard Hardin, Christoph Beckermann - *University of Iowa*
Laura Bartlett - *Missouri University of Science and Technology*
Robin Foley, John Griffin, Charles Monroe - *University of Alabama at Birmingham*

Introduction

Investment castings are commonly considered to have fewer issues with inclusions (reoxidation). On one hand, this seems counterintuitive given that the pouring and gating for a typical investment casting involves metal rapidly being poured down a long, large sprue (tree) and then oftentimes filling the mold cavity with additional "waterfalls". Thus, it would seem that the increased opportunity for interaction between the molten steel and air would promote the formation of inclusions. That said, typical investment castings do offer some opportunities. Wall sections are generally thin and quick to solidify, which would limit time for inclusions to agglomerate and float up. In addition, the ceramic shell of an investment casting is sintered and provides an inert atmosphere unlike sand castings where mold-metal reaction must be managed.

Based upon on-going SFSA research and continued efforts by SFSA members to develop process improvements, a SFSA team of members and researchers began to discuss opportunities for utilizing a naturally pressurized gating system for investment castings. As of early 2019, those involved were only aware of one instance where a foundry utilized bottom gating of an investment casting, but not truly a naturally pressurized gating design for investment castings.

The team discussed factors that need to be considered in developing a naturally pressurized gating system. Unlike in traditional investment casting rigging where it has a center tree / sprue that also acts as the riser, we needed to consider having a separate sprue and a feeder. The sprue, runner, and gates must be sized properly to eliminate any opportunity for air aspiration. One method to minimize air entrainment is the use of a surge cylinder in the runner [1,2]. The in-gate into the surge cylinder must be tangential to the runner to create a vortex flow. The idea is to prevent the metal stream rolling back to the runner and instead get the stream to climb the walls of the cylinder. It would also capture the leading metal front and contain the "damaged" metal. The rigging system must be completely filled before the metal stream enters the in-gates.

University of Northern Iowa and University of Iowa collaborated in developing a naturally pressurized gating system. Initial design had a main sprue and a separate tree acting as a riser. It also incorporated a surge cylinder at the end of the runner and an up-gate cylinder. This initial design had a filter before the metal enters the up-gate; however, the team decided to not use filters based on previous filling issues experienced by the foundry with the alloy being used. Based on inputs from the team, the rigging was resized to improve filling and minimize air entrainment. Two naturally pressurized (NP) gating systems were eventually proposed (details provided in the next section).

The NP gating systems were evaluated through modeling and casting trials. They were compared to traditional investment casting rigging systems. In this study, the alloy used was a high aluminum

manganese steel. The alloy has gained much interest as a lightweight alternative to quench and tempered Cr and Mo martensitic steels for military and commercial vehicles. Adding aluminum decreases the density of the manganese steel up to 18% when compared to traditional high strength steels.[3-6] Typical alloy compositions contain 20-30%Mn, 5-11% Al, and 0.3-1.0%C, and are age hardenable resulting from homogenous precipitation of κ-carbide within the austenite matrix.[4, 7-10] An austenitic matrix and high work hardening rates contribute to excellent combinations of strength and toughness. However, the toughness of these steels has been shown to be dependent on the type and distribution of non-metallic inclusions. As a result of the high aluminum content, these steels tend to be very "drossy" and they are prone to forming AlN inclusions and oxide bi-films during melting and casting. In a recent study by Schulte et al. they have shown that a high density of AlN inclusions can decrease the notch toughness of the alloy by as much as 50%.[11] It was therefore decided that a casting made in this alloy would be ideal as a case study for this project. A member foundry is currently producing an investment cast shoe in the alloy; thus, tooling for these castings was also readily available. Figure 1 shows an example of the as-cast shoe.

Figure 1. As-cast high aluminum manganese steel shoe.

Modeling

The air entrainment and inclusion models developed at the University of Iowa were utilized to evaluate three different gating systems for the investment castings [12]. The gating system used to commercially produce the shoe castings underwent several design iterations. The modeling comparison in this section is between the two naturally pressurized (NP) rigging systems and only one of the earlier versions of a traditional investment rigging. The following section on the casting trials describes the other investment casting gating systems that were evaluated experimentally.

The traditional investment rigging and the two naturally pressurized, NP, systems were each treed with two shoes. The traditional tree has a central sprue which both acts as a sprue and as a riser (Figure 2a). The sprue feeds each shoe through a thick runner and vertical in-gates running along the vertical flat faces of each casting. There is a flow-off at the top of each shoe casting.
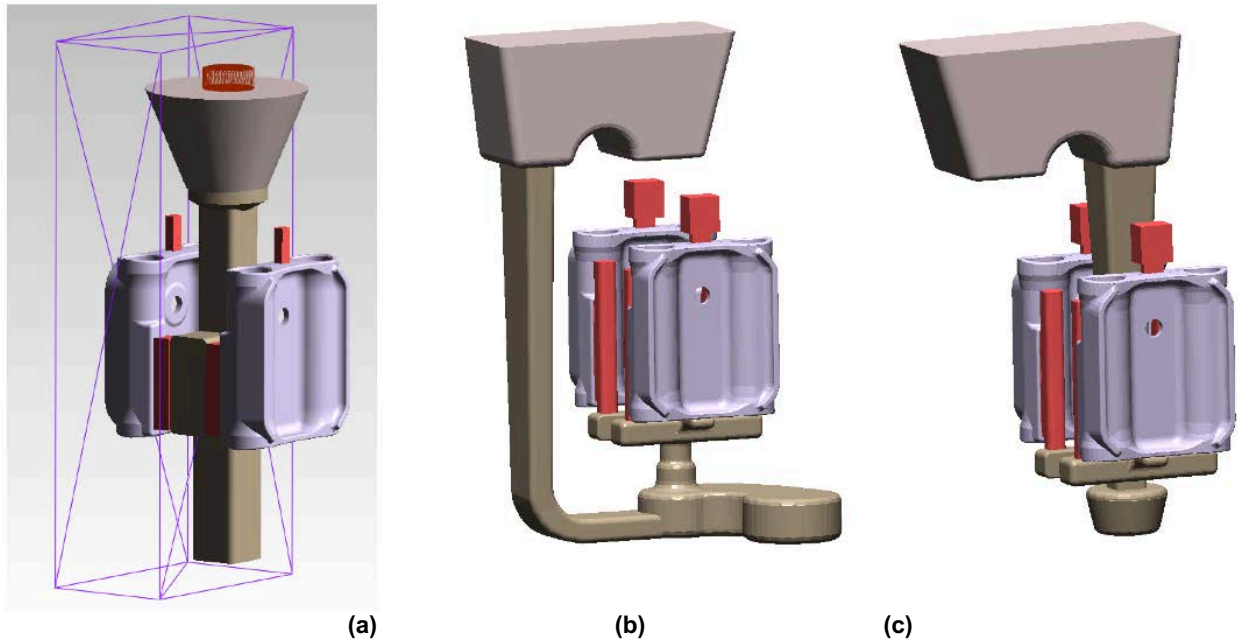
Figure 2. (a) Traditional investment casting tree and (b) naturally pressurized rigging system with side sprue and (c) with center sprue

Shown in Figures 2 (b) and (c) are the NP gated shoe castings. Figure 2 (b) shows a NP gating system that also contains a traditional center tree acting as a riser, however, this system has a separate side sprue where the metal flows down and fills the casting from the bottom. The side sprue is tapered to accommodate the constriction of the metal stream. The center sprue / tree from the traditional rigging was kept in this NP gating system to help catch inclusions as shown in Figure 2 (b). A cylindrical in-gate was added at the bottom and there was a flow-off at the end of the runner. The vertical in-gates were made taller, however, they have the same area as the in-gates of the traditional rigging to collect inclusions and provide feed metal. The flow-off at the top of the shoes was also made larger to help feed the shrinkage in the area near the mounting hole and to help trap inclusions.

The second NP rigging system was similar to the traditional tree because of the large center sprue. This sprue, however, was tapered so that it filled more quickly and the runner was made thinner, as shown in Figure 2 (c), than the traditional rigging. A sprue well was located at the bottom to capture the inclusions formed during the initial filling of the sprue. The vertical in-gates in Figure 2 (c) were similar to the other NP gating system, Figure 2 (b). Figure 2 (c) also incorporates a flow-off / mini-riser at the top of each shoe. The NP in Figure 2 (c) was designed to have a better yield than the NP with side sprue by eliminating the additional features at the bottom of NP with side sprue.

The two NP gating systems used an offset pouring basin, which would allow inclusions to float up before the metal stream flows through the sprue. The cylindrical step or weir in the offset basin slows down the metal stream as it enters the sprue which results to a lower flow velocity at the base of the sprue. The predicted fill time was 4 seconds for the traditional investment tree, Figure 2 (a), 4 ½ seconds for the NP with center sprue Figure 2 (c), and 6 seconds for the NP with side sprue, Figure 2 (b). For the NP with side sprue, the sprue system is completely filled by the time the metal enters the cylindrical in-gate.

Figure 3 illustrates the predicted entrained air in the traditional rigging and the two NP systems. The traditional investment rigging has over five times more entrained air volume than the two NP systems. This is as expected since the offset pouring basin in the NP systems gives more time for the entrained air to escape before the metal enters the sprue. The NP with the side sprue has the least amount of entrained air.
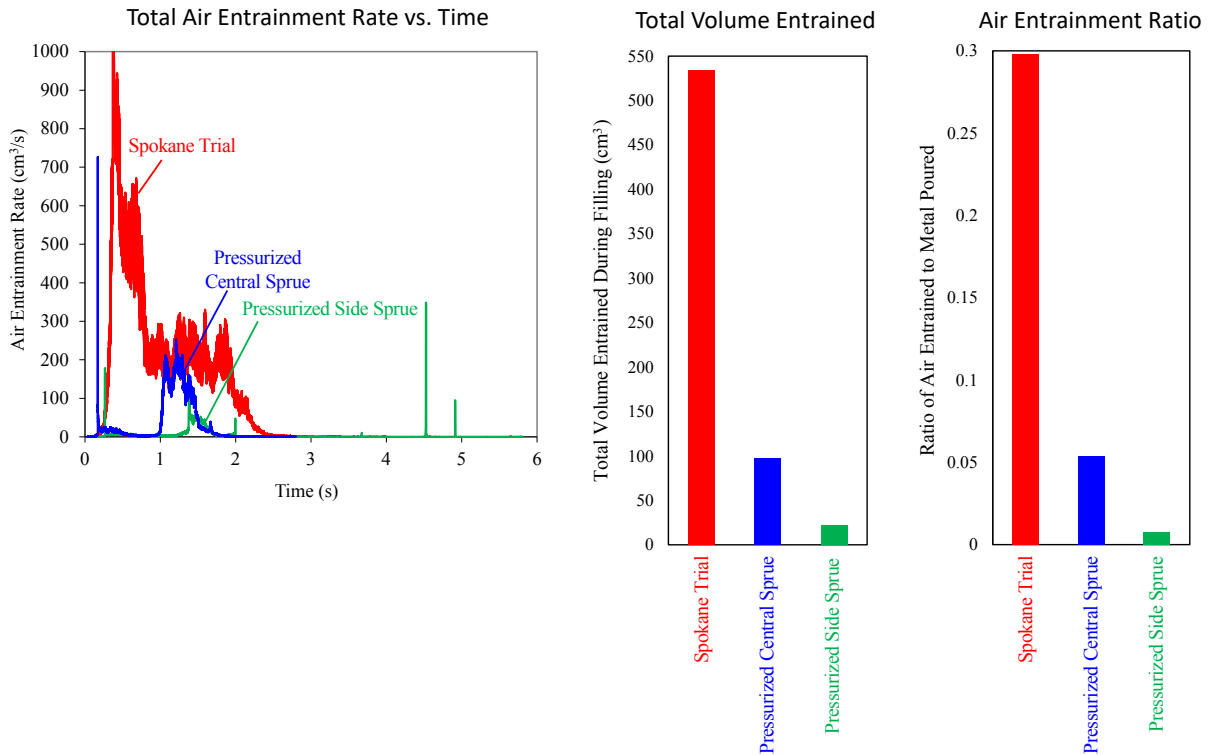

Figure 3. Predicted air entrainment for the traditional investment casting tree (red) in comparison with the naturally pressurized gating system with a center sprue (blue) and the naturally pressurized gating system with a side sprue (green).

Figure 4 compares the final inclusion particle size distribution in these three gating systems. As expected based on the air entrainment simulation results, the traditional gating system has more numerous and larger inclusions in the casting compared to the two NP systems. Note that inclusions were caught by the vertical in-gates in both NP systems. It can be noticed that there are no predicted inclusions near the mini-riser / flow-off at the top of the two NP gating.
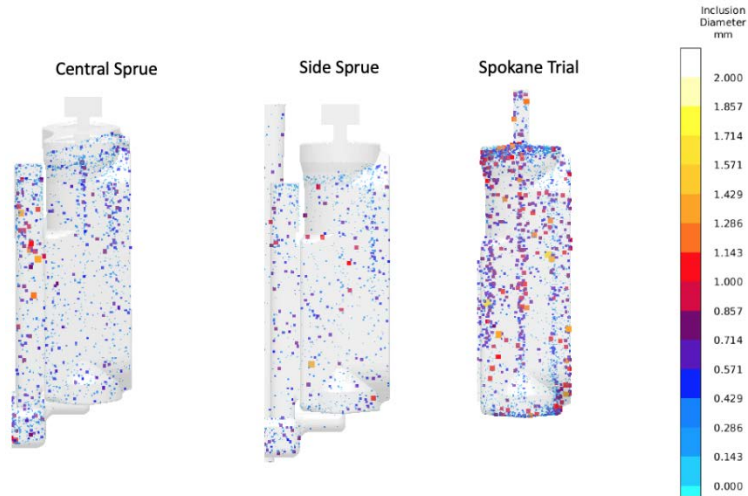
Figure 4. Predicted inclusion size distributions for traditional investment casting tree vs naturally pressurized with center sprue vs naturally pressurized with side sprue

Casting Trials

The naturally pressurized gating systems were compared with several traditional investment casting rigging which underwent several iterations as the foundry was trying to optimize their production method of the shoes. Not all of these iterations were used in the casting trials including the traditional investment tree modeled in the previous section. Table 1 summarizes the different rigging systems.

Table 1. List of Different Gating Systems for Investment Castings

Casting ID	Gating System	Description	Figure Number
1	#1	Pin bore holes horizontal (only horizontal in-gates)	Figure 5a
2	#2	Pin bore holes vertical, not bottom gated (only vertical in-gates)	Figure 5b
3 3X	#3	Pin bore holes vertical, bottom gated (vertical in-gates + bottom center in-gate)	Figure 6a
4 4X	#4	Pin bore holes vertical, not bottom gated, modified vertical in-gates	Figure 6b
5 5X	#5	Pin bore holes vertical, bottom gated, modified vertical in-gates (similar to #4 but vertical in-gates are positioned higher)	Figure 7
S1X* S2X	Naturally Pressurized (NP) with side sprue	-	Figure 9
C1X C2X	Naturally Pressurized (NP) with center sprue	-	Figure 10

S1X casting was not included in tensile and inclusion analysis

The first rigging system (#1) was treed with only 1 shoe (Figure 5a). The shoe was oriented horizontally (the pin bore holes were horizontal). The shoe was fed through horizontal in-gates along the flat faces. The shoe was then oriented vertically in the second rigging system (#2) as shown in Figure 5b. It has vertical in-gates along the flat faces. It was actually treed for 2 shoes but the 2nd casting did not fill due to wax/shell issue.

Figure 5. Traditional investment gating systems (a) #1 and (b) #2

The next rigging system (#3) had vertical in-gates and an additional bottom center in-gate (Figure 6a). It was treed for 2 shoes. The vertical in-gates were modified in rigging #4 and the bottom center in-gate was removed (Figure 6b). It also was treed for 2 shoes.

Figure 6. Traditional investment gating systems (a) #3 and (b) #4

The last iteration (#5) has the same modified vertical in-gates as #4 but the position of in-gates in #5 is higher to make room for a bottom center in-gate (Figure 7). Gating systems #3 and #5 have the same size bottom center in-gate. Gating #5 was treed with 2 shoes. Figure 8 has the gating #3, #4, and #5 side-by-side to show how their vertical in-gates and bottom center in-gates compare with one another.

Figure 7. Traditional investment gating system #5

Figure 8. Comparison of traditional investment gating systems #3, #4, and #5

Figure 9 and Figure 10 show the rigging and the shoes for the 2 naturally pressurized gating systems. One tree was poured for each gating system. All castings were poured from the same heat. The pour times for the non-pressurized gating systems were 7 to 9 seconds. The pour time for the NP with side sprue was 11 seconds while for NP with center sprue was 10 seconds. The pourer may have contributed to pour time variability. Visually, the NP gating system shoes looked best followed closely by traditional gating system #5.

Figure 9. Naturally pressurized (NP) with side sprue

Figure 10. Naturally pressurized (NP) with center sprue

Figure 11 to Figure 17 show the castings for the different rigging systems after solution heat treatment. All castings were visually inspected and radiographed.

Figure 11. Casting after heat treatment for traditional investment gating system #1

Figure 12. Casting after heat treatment for traditional investment gating system #2

Figure 13. Castings after heat treatment for traditional investment gating system #3

Figure 14. Castings after heat treatment for traditional investment gating system #4

Figure 15. Castings after heat treatment for traditional investment gating system #5

NOTE: S 1X casting is missing so this will not be included in tensile and inclusion analysis

Figure 16. Castings after heat treatment for naturally pressurized with side sprue

Figure 17. Castings after heat treatment for naturally pressurized with center sprue

The RT results for the traditional investment gating systems and the 2 NP rigging are in Figure 18. Radiographic testing was not required for this casting, but type and level were noted. In general, most of the castings regardless of rigging method show some shrink.
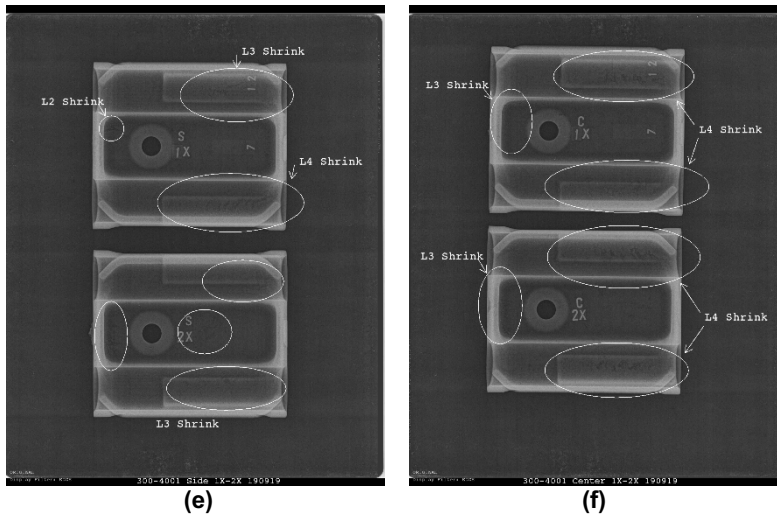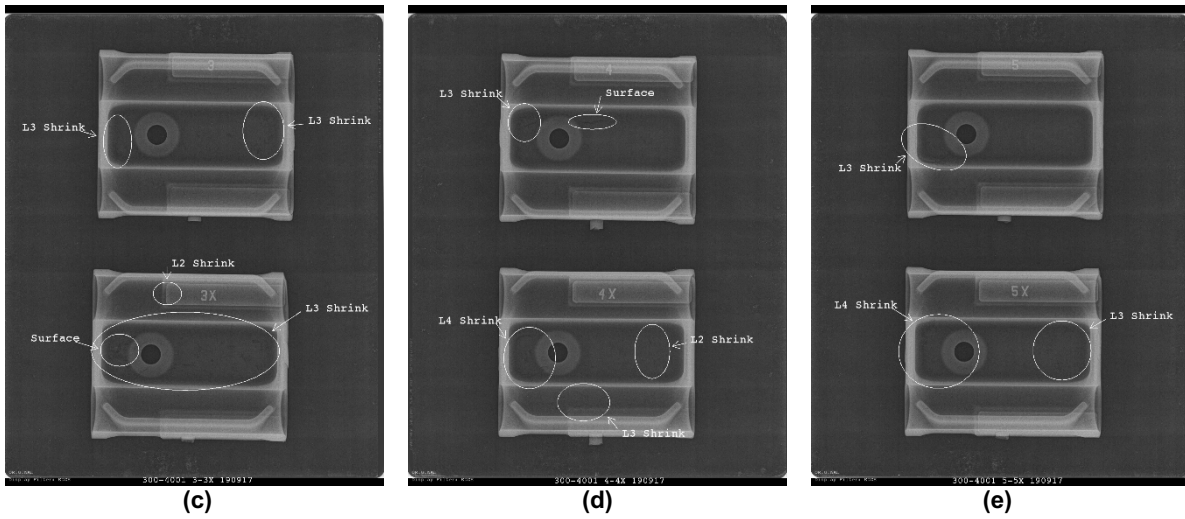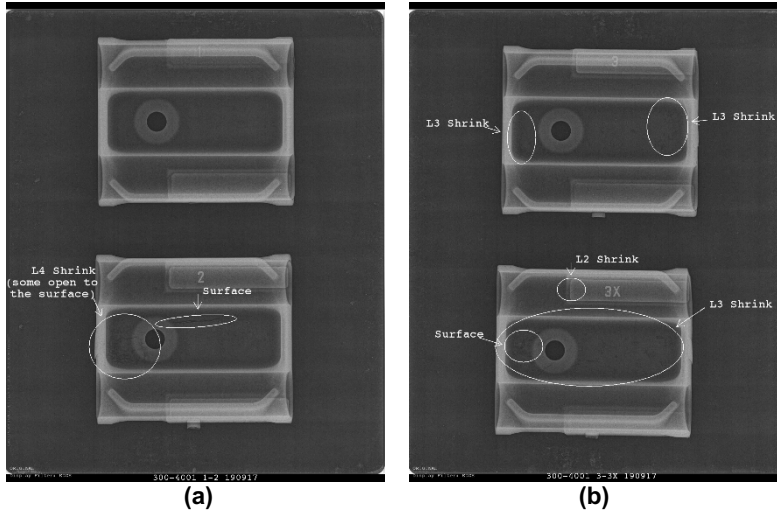
Figure 18. Radiography test results for traditional investment casting gating (a) #1, (b) #2, (c) #3, (d) #4, (e) #5 and naturally pressurized gating system with (e) side sprue and (f) center sprue. Note that casting S1X was not included in tensile and inclusion analysis.

Tensile Testing

Three tensile specimens were sectioned from each casting (Figure 19). The locations where tensile specimens could be taken from were limited by the wall thickness of the shoe. Tensile test results were not available at time of publication.

Figure 19. Tensile specimen locations in each shoe

Inclusion Analysis

The naturally pressurized (NP) casting with a side sprue (S2X) and the naturally pressurized (NP) casting with the center sprue (C2X) were sectioned for optical metallography and inclusion analysis as shown in Figure 20.   Figure 21 (a) shows an optical micrograph of a large oxide bi-film found in the S2X casting. These bi-films were composed mainly of alumina as shown in Figure 21 (b). Both NP castings showed significant bi-films in the areas of analysis that covered as much as 25% of the total specimen area. In some cases, secondary cracking was noted at the ends of bi-films that may have formed during fast cooling from quenching. Bi-films were also shown in some cases to nucleate AlN plates during cooling after solidification, perhaps during subsequent heat treatment. Inclusion analysis was performed using an ASPEX PICA 1020 scanning electron microscope, SEM, with Automatic Feature Analysis (AFA) software and equipped with a backscattered electron detector (BSED) and an energy dispersive X-ray spectroscopy (EDS) detector. Inclusions were classified into four different groups: AlN, AlN-MnS, MnS, and additional nitrides. It should be noted that the "additional nitrides" are also small AlN or AlN-MnS complex inclusions which the background Mn content from the interaction volume complicates the ability of the rule file to accurately classify these inclusions. A representative backscattered electron (BSE) image of an AlN and a complex AlN-MnS inclusion are shown in Figures 22 (a) and (b), respectively. AlN was the most common inclusion observed in the castings. AlN forms above the liquidus in this alloy and is present during melting and casting. MnS forms at a lower temperature below the liquidus during solidification and will often use pre-existing AlN as a heterogeneous nucleation site. This creates the complex AlN-MnS inclusions that are most often observed in these steels. Oxides present in the steel were tied up as bi-films and not discrete inclusions.

(a)   (b)

Figure 20 (a) The castings were sectioned for inclusion analysis in the two areas (left and right) denoted by the highlighted regions. These areas were shown by inclusion modeling to have the highest concentration of inclusions. (b) Sectioning plane showing the exact location of the inclusion analysis highlighted in red.
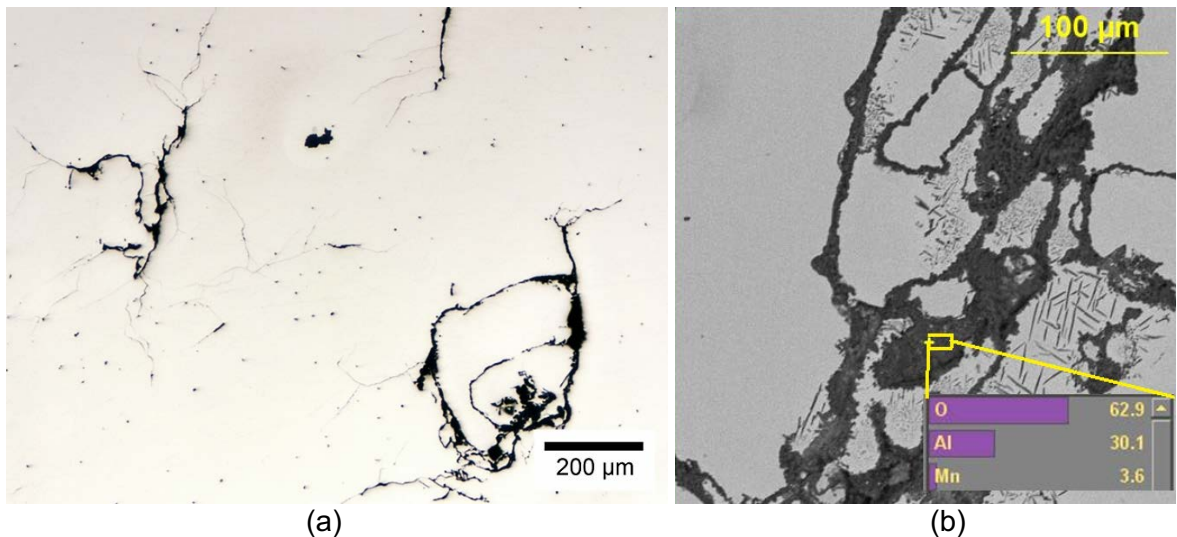

(a)   (b)

Figure 21 (a) Large bi-films in the naturally pressurized (NP) casting with a side sprue (S2X). (b) EDS analysis confirmed that these bi-films were mainly alumina. AlN plates are shown to nucleate from bi-films during cooling after solidification or during subsequent heat treatment.
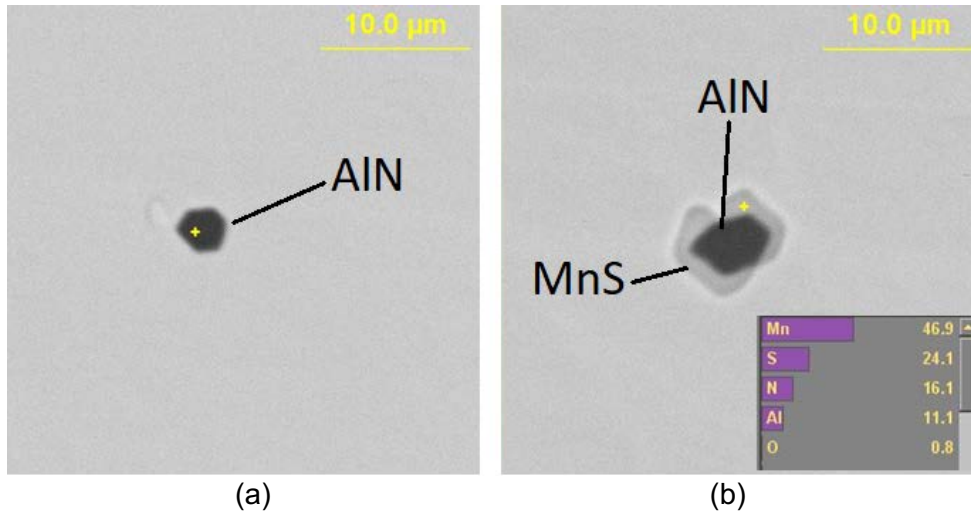
Figure 22 (a) Inclusions in the alloy were mainly AlN that forms above the liquidus and during steelmaking. (b) During solidification, MnS will precipitate on pre-existing AlN forming complex AlN-MnS inclusions. The typical chemistry of the AlN-MnS inclusions is given in (b).

Figure 23 (a) shows the inclusion density by type and Figure 23 (b) shows the area fraction of inclusions by type. Inclusion analysis of the two NP castings showed a slight reduction in the amount and area coverage of inclusions in the naturally pressurized (NP) casting with a side sprue (S2X) when compared with the in the naturally pressurized (NP) casting with the center sprue (C2X). The size distribution of AlN and AlN-MnS inclusions was largely the same between the two castings and most inclusions were between 3 and 5 microns in average diameter.
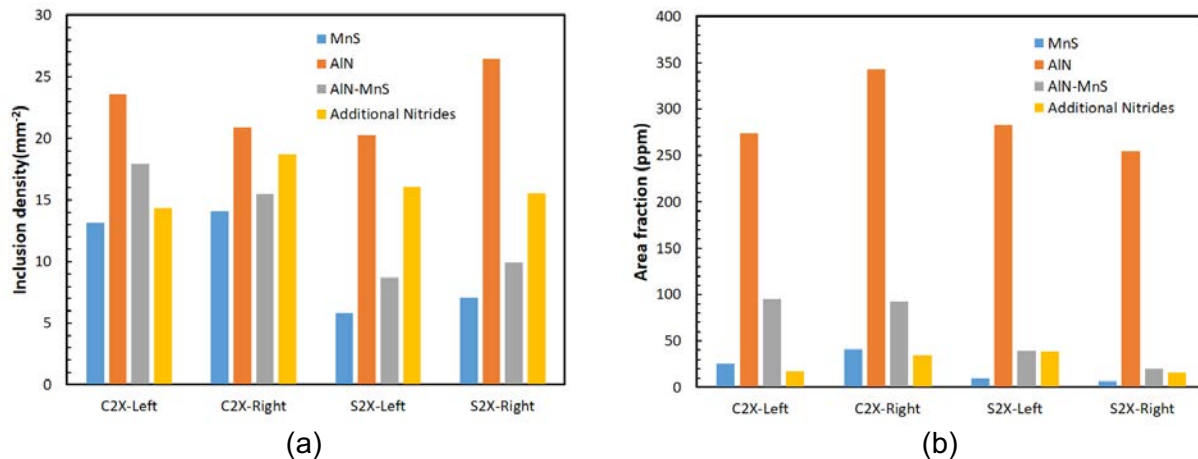

Figure 23. (a) Inclusion density by type and (b) area fraction of inclusions by type. Inclusion analysis of the two NP castings showed a slight reduction in the amount and area coverage of inclusions in the naturally pressurized (NP) casting with a side sprue (S2X) when compared with the in the naturally pressurized (NP) casting with the center sprue (C2X).

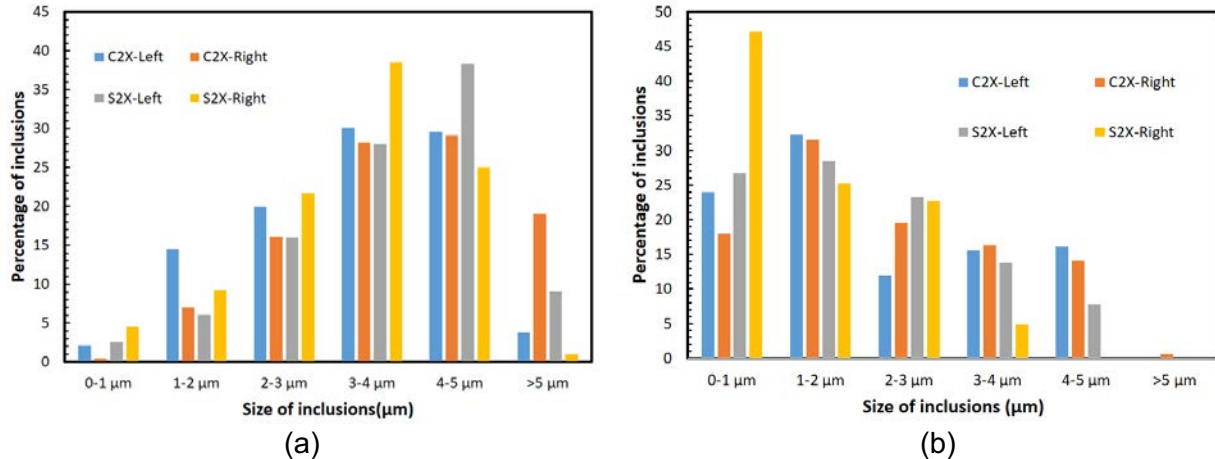(a)   (b)

Figure 24. (a) Size distribution of AlN and (b) AlN-MnS inclusions. (a) Both castings had similar inclusion size distributions with most inclusions between 3 and 5 microns in average diameter.

Conclusions

At the time of publication, many of the test results were not yet available. Tensile properties for the shoes, analysis and characterization of tensile specimens, and inclusion analysis of the shoes and gating system will be done. Visual inspection of the castings by both the foundry and universities who are familiar with the alloy identified that the naturally pressurized (NP) rigging systems appeared to have good surface quality compared to traditional gating systems for investment castings, which would correlate to the modeling prediction for reduced air entrainment and inclusions for NP gating systems. Preliminary inclusion analysis was only done in two areas for only the two NP gating systems. The majority of the inclusions present in the naturally pressurized castings were AlN and complex AlN-MnS. Significant oxide bi-films, which were mainly composed of alumina, were also prevalent in the evaluation areas. The NP system with the side sprue had less and smaller inclusions compared to the NP with the center sprue. Again, further inclusion analysis will be done to fully characterize the two NP gating systems and the various traditional gating systems for investment castings.

Acknowledgements

Disclaimer

The publication of this material does not constitute approval by the government of the findings or conclusion herein. Wide distribution or announcement of this material shall not be made without specific approval by the sponsoring government activity.

References

[1] J. Plunger, "Air Entrainment: Testing the Model", SFSA T&O Conference 2017, Paper 3.4

[2] W. Marquardt, "Continuing the Conversation Naturally Pressurized Fill System", SFSA T&O Conference 2018, Paper 4.11

[3] R. A. Howell, J.S. Montgomery, D.C. Van Aken, "Advancements in Steel for Weight Reduction of P900 Armor Plate," AIST Trans. 6 (5), pp. 168-176 (2009).

[4] G.L. Kayak, "Fe-Mn-Al Precipitation Hardening Austenitic Alloys," Met. Sc. And Heat Tr., vol. 11, pp. 95-97 (1969).

[5] Kalashnikov, I.S., Acselrad, O., Shalkevech, A., Chumokova, L.D. Pereira, L.C., "Heat Treatment and Thermal Stability of FeMnAlC Alloys," Journal of Materials Processing Technology, vol. 136, pp. 72-79 (2003).

[6] Sato, K., Igarashi, Y. Inouue, Y. Yamazaki, T., Yamanaka, M., "Microstructure and Age Hardening in Spinodally Decomposed Austenitic Fe-Mn-Al-C Alloys," Proceedings of the International Conference on Stainless Steels (1991).

[7] Howell, R.A., Weerasooriya, T., and Van Aken, D.C., "Tensile, High Strain Rate Compression and Microstructural Evaluation of Lightweight Age Hardenable Cast Fe-30Mn-9Al-X Si-0.9C-0.5Mo Steel," Transactions of the American Foundry Society (2008).

[8] Frommeyer, G., Brux, U., "Microstructures and Mechanical Properties of High Strength Fe-Mn-Al-C Lightweight TRIPEX Steels" Steel Research International vol. 77, pp. 627-633 (2006)

[9] Choo, W.K., Kim, J.H., "Microstructure and Mechanical Property Changes on Precipitation of Intermetallic K' in the Fe-Mn(Ni)-Al-C Solid Solution" Conf. on ThermoMechanical Processing of Steels and Other Materials, pp. 1631-1637 (1997).

[10] Sato, K., Tagawa, K., Inoue, Y., Modulated Structure an d Magnetic Properties of Age Hardenable Fe-Mn-Al-C Alloys", Met. Trans. A. Vol. 21A, pp. 5-11 (1990)

[11] Schulte, A.M., Lekakh, S.N., Van Aken, D.C., Richards, V.L., "Phosphorus Mitigation in Cast Lightweight Fe-Mn-Al-C Steel, " 114th Metalcasting Congress, Orlando, FL, March 19-20 (2010).

[12] Majidi, S.H., and Beckermann, C., "Modelling of Air Entrainment During Pouring of Metal Castings," Int. J. Cast Metals Research, Vol. 30, 2017, pp. 301-315.